First Measurements of the Toroidal Rotation of the Bulk Ions at TEXTOR by Rutherford Scattering

H. F. Tammen,[1] A. J. H. Donné,[1] H. Euringer,[2] and T. Oyevaar[1]

[1]*FOM-Instituut voor Plasmafysica "Rijnhuizen," Association EURATOM-FOM, P.O. Box 1207, 3430 BE Nieuwegein, The Netherlands*

[2]*Institut für Plasmaphysik, Forschungszentrum Jülich GmbH, Association EURATOM-Kernforschungsanlage, P.O. Box 1913, 52425 Jülich, Germany*

(Received 16 August 1993)

The Rutherford scattering diagnostic at TEXTOR was used to determine the central toroidal rotation speed of the hydrogenic bulk ions in the plasma. During neutral beam injection speeds of the order of 10^5 ms^{-1} were found. With balanced injection no rotation was observed. A first comparison with charge exchange recombination spectroscopy showed, within the accuracy of the methods, no difference in the derived speeds, in agreement with neoclassical theory. The momentum confinement time of the central hydrogenic ions was found to decrease with the neutral beam power as approximately $1/\sqrt{P_{\mathrm{NBI}}}$.

PACS numbers: 52.50.Gj, 52.55.Fa

The toroidal rotation speed (v_ϕ) of a tokamak plasma is associated with a number of interesting aspects of tokamak physics. Especially impurity transport is generally believed to be strongly correlated with toroidal plasma rotation. It has, e.g., been observed at various tokamaks where the injection of fast, neutral particles (NBI) parallel to the plasma current (coinjection) suppresses the accumulation of impurities in the center of the plasma, while in the case of counterinjection the impurity buildup is enhanced [1,2]. Usually, v_ϕ is measured by active charge exchange recombination spectroscopy (CXRS) [3–5]. With this technique the rotation is inferred from the spectral shift of impurity line emission, i.e., the Doppler shift. The impurities involved are mainly C or O, but heavier elements are also used. Typical speeds measured during NBI are of the order of 10^5 ms^{-1}. With (near) balanced injection hardly any or no rotation is observed.

To be able to compare experimental results with predictions from various theoretical models, it is often assumed that the rotation speed of the hydrogenic bulk ions ($v_{\phi,i}$) equals that of the impurity ions ($v_{\phi,I}$). There are, however, results from neoclassical theory which indicate that this need not always be the case [6,7]. Therefore, measurements of $v_{\phi,i}$, alongside $v_{\phi,I}$, are desirable. As is shown below, these can be performed by the Rutherford scattering diagnostic (RUSC) at TEXTOR.

The differential cross section for Rutherford scattering on a Maxwellian ion velocity distribution with a temperature T_i and shifted to a drift velocity $v_{0\parallel}$ is given by

$$\frac{d\sigma}{d\Omega} = \frac{u_b^3}{v_b|\mathbf{u}_b-\mathbf{v}_b|^5}\left[\frac{Z_pZ_be^2}{2\pi\varepsilon_0 m_b}\right]^2\left(\frac{m_p}{2\pi T_i}\right)^{1/2} \times\exp\left(-\frac{m_p(v_{p\parallel}-v_{0\parallel})^2}{2T_i}\right), \quad (1)$$

where Z_b and Z_p are the charge numbers and m_b and m_p the masses of the beam and plasma particles, respectively [8]. The velocities of the beam particles before and after scattering are represented by $\mathbf{v}_b$ and $\mathbf{u}_b$, and $v_{p\parallel}$ is the velocity component of the plasma particle before scattering in the direction parallel to $\mathbf{u}_b-\mathbf{v}_b$. Several conclusions can be drawn from Eq. (1). First, the information contained in the energy distribution of the observed scattered particles relates to the velocity distribution in one well-defined direction. Second, bulk motion of the plasma ions in the direction of observation shows up as a shift of the complete spectrum of the scattered particles. And third, the width of the energy distribution of the scattered particles is strongly correlated with the temperature of the plasma ions.

This principle is used by the Rutherford scattering diagnostic [9,10] at TEXTOR [11] to perform spatially and temporally resolved measurements on the ion velocity distribution of the thermonuclear plasma (see Fig. 1). A narrow beam of monoenergetic, neutral He particles (10 mA, 30 keV) is injected vertically into the plasma. A small part of the beam particles collides elastically with the moving plasma ions and is scattered in the forward direction. The energies of the scattered particles are determined by means of a time-of-flight analyzer at a certain, adjustable angle (3°–8°) and their distribution carries information about the ion velocity distribution inside the scattering volume, which is defined by the intersection of the He beam and the line of sight of the analyzer. The present geometry of RUSC is such that the scattered particles carry information about the ion velocity distribution parallel to the toroidal magnetic field, so $v_{0\parallel}$ can be identified with $v_{\phi,i}$. A typical example of a recorded time-of-flight spectrum during an Ohmic discharge is given in Fig. 2, together with the instrumental function, to illustrate the broadening which occurs due to the thermal movement of the plasma ions. Function parametrization techniques are used for data analysis [12].

It should be noted that in spite of the dependence of $d\sigma/d\Omega$ on Z_p^2 (the dependences on T_i and m_p disappear when calculating the total scattering yield by integrating $d\sigma/d\Omega$), the effect of impurities in the plasma on the

0031-9007/94/72(3)/356(4)$06.00

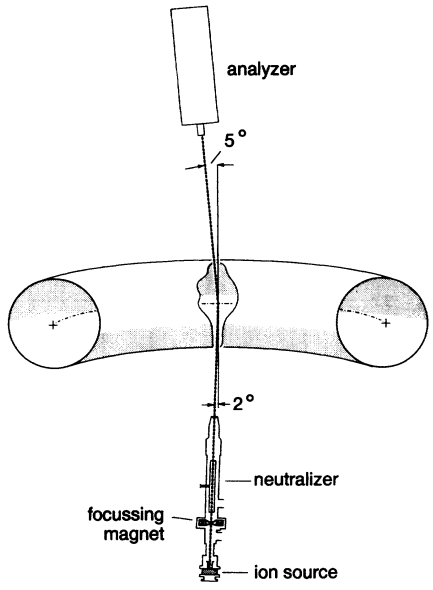

FIG. 1. Schematic view of the experimental setup of the Rutherford scattering diagnostic at TEXTOR.

measurements is negligibly small. This is due to two effects. First, the scattering yield is proportional to the ion density in the scattering volume, which is much smaller for impurities than for the bulk ions. Second, a number of beam particles becomes ionized during the scattering process. These ionized particles are trapped in the magnetically confined plasma and are thus not observed by the analyzer. As the probability for ionization of the probing beam particles is much larger for scattering on impurities than for scattering on H or D [13], an upper limit of only 5% can be deduced as the percentage of the spectrum which is composed of particles that have been scattered on impurities.

Simulations using the parameters of RUSC indicated that toroidal rotation speeds $> 10^4$ ms^{-1} should be observable at TEXTOR. First attempts to observe $v_{\phi,i}$ in this way were made during the latest measuring campaign at TEXTOR. Several discharges with NBI were monitored. The time evolutions of plasma current, line-averaged electron density, electron temperature at $r = -7$ cm (the center of the plasma was at $r = 6$ cm), and NBI power of one of these discharges are shown in Fig. 3. For experimental reasons not discussed here, the toroidal field was 1.8 T instead of the usual 2.25 T. Hence, no electron cyclotron emission channel could be set at the center of the plasma. The central electron temperature (T_e) is estimated to be 20%–25% higher than the displayed one, based on similar shots with "normal" toroidal field. The scattering angle of RUSC was 7° and the scattering volume was positioned at the center of the plasma.

Several characteristics of the data, collected during the same discharge as in Fig. 3, are given in Fig. 4. They are (a) the number of detected counts in a spectrum, (b) the position of the center of a spectrum, and (c) the width of

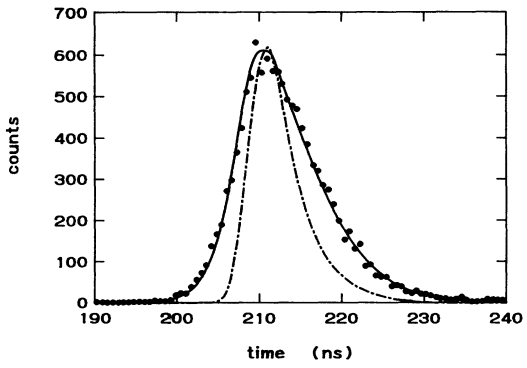

FIG. 2. Typical example showing the broadening of the time-of-flight spectrum as compared to the instrumental broadening. The beam energy was 30.1 keV and the scattering angle 7°. For this discharge a central ion temperature of 1.0 ± 0.1 keV was deduced.

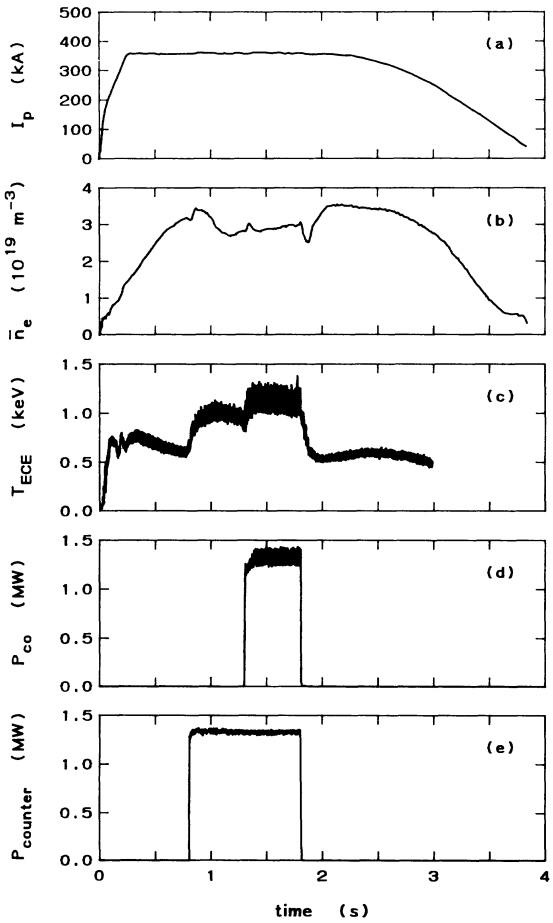

FIG. 3. Time evolution of plasma current (a), line-averaged electron density (b), electron temperature at $r = -7$ cm (c), NBI-co power (d), and NBI-counter power (e).

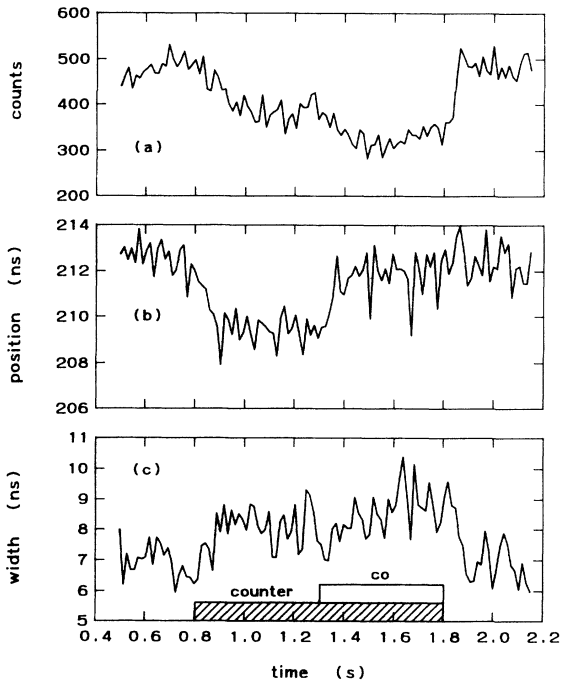

FIG. 4. Number of detected counts (a), position of the center (b), and width (c) of spectra collected during the same discharge as displayed in Fig. 3.

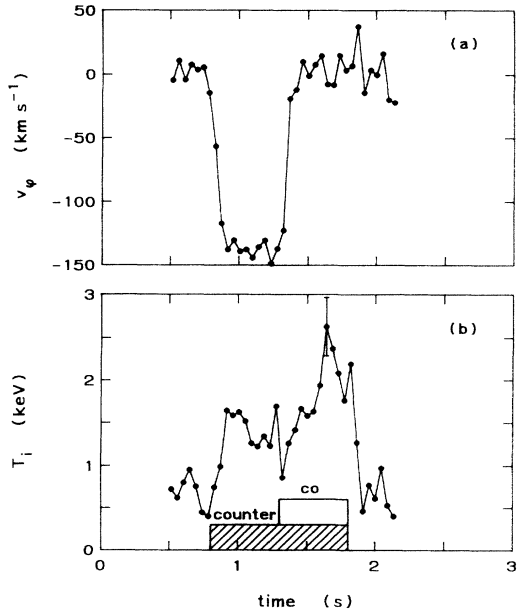

FIG. 5. Ion temperature (a) and toroidal rotation speed (b) obtained with the Rutherford scattering diagnostic for the same discharge as displayed in Fig. 3.

a spectrum. The total integration time per spectrum was 15 ms. A number of observations can be made. First, a change in the counting rate of the diagnostic can be seen after NBI is switched on/off. This is caused by enhanced losses of the diagnostic beam due to the changing edge layer of the plasma during the NBI. Second, the complete time-of-flight spectrum shifts to smaller values when the NBI-counter is switched on. This is caused by the toroidal rotation of the plasma. With balanced injection, only a small shift remains, which disappears once both beams are switched off. Third, the use of NBI leads to a substantial increase in the width of the spectrum, reflecting a higher ion temperature of the plasma.

Having established qualitatively that toroidal rotation can indeed be observed, a quantitative estimate of $v_{\phi,i}$ can now be made. Rotation during Ohmic heating alone appears to be very small at TEXTOR ($\leq 10^4$ ms^{-1}), as can be concluded from $n=1$ MHD mode frequencies. Consequently, the average position of spectra obtained during the Ohmic phase of a discharge can be used as a reference zero level, as it is below the detection threshold of RUSC. It should also be noted that the spectral position is a (weak) function of T_i: The efficiency of the RUSC analyzer is better for higher energies, so the spectrum for a high T_i will be weighted towards shorter flight times, compared to a low T_i. The shift of the spectrum which occurs after the onset of NBI, taking this effect into account, can now be used to deduce $v_{\phi,i}$, as compared to the Ohmic phase. In this way a speed of $1.4(\pm 0.2) \times 10^5$ ms^{-1} has been deduced during NBI-counter for this discharge. During balanced injection the spectrum is slightly shifted (≈ 0.6 ns) with respect to the Ohmic phase, but this shift can be attributed to the dependence on T_i. It can therefore be concluded that $v_{\phi,i}$ during balanced injection equals $v_{\phi,i}$ during Ohmic heating. The time evolutions of both $v_{\phi,i}$ and T_i are presented in Fig. 5. It should be noted that three spectra were added to improve the statistics, so the integration time of a spectrum was artificially increased to 45 ms. T_i varies from about 0.7 keV in the Ohmic phases of the discharge to 1.4 keV

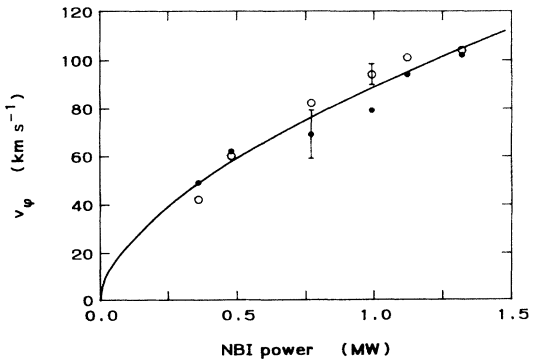

FIG. 6. Central toroidal rotation speed of the bulk ions by Rutherford scattering (closed circles) and that of carbon by charge exchange recombination spectroscopy (open circles) during an NBI-power scan. Both ion species have, within the accuracy of the methods, the same speed. The fit shown is proportional to $(P_{NBI})^{0.58}$.

during the NBI-counter and 2.0 keV during balanced injection. The values obtained in the Ohmic phases are close to the (estimated) T_e, but during NBI T_i is somewhat higher than T_e.

Finally, a first investigation into the dependence of $v_{\phi,i}$ on the injected NBI power (P_{NBI}), using the NBI-co injector, and a comparison with $v_{\phi,I}$ were made. One of the ten horizontal sight lines of the CXRS diagnostic was used to infer $v_{\phi,I}$ of C by measuring the Doppler shift of the C VI 529.05 nm line. The main plasma and diagnostic parameters were similar to the ones mentioned above. P_{NBI} was not varied by changing the injection energy of the particles, but by reducing the number of injected particles. In this way the penetration depth of the beam was kept constant for all discharges. The results of the scan are given in Fig. 6, where $v_{\phi,i}$ and $v_{\phi,I}$ are plotted versus P_{NBI}. The rotation is clearly seen to increase in a nonlinear way with P_{NBI}. Within the error bars both speeds display a similar behavior. A simple power fit revealed that v_ϕ is, within statistical uncertainties, almost proportional to $\sqrt{P_{\mathrm{NBI}}}$ for the limited data set under consideration: An exponent of 0.58 was found. This implies that the momentum confinement time for the hydrogenic ions in the interior of the plasma (τ_m), which can be defined as the average central particle momentum divided by the toroidal momentum deposited from the beams, decreases approximately as $1/\sqrt{P_{\mathrm{NBI}}}$. This scaling of τ_m with P_{NBI} is similar to the one for the energy confinement time in the L mode. Similar observations were reported at ISX-B [4] and JT60 [14]. Expansion of the data set will allow a statistically more reliable statement about the exact dependence.

The similarity of $v_{\phi,i}$ and $v_{\phi,I}$ has been compared with theoretical predictions by Kim, Diamond, and Groebner [7]. In their article, they derive from neoclassical theory expressions for the toroidal speed of both species. For the experimental conditions under consideration, the toroidal rotation of both ion species is driven by the radial electric field, but the rotation of the hydrogenic ions is dampened by ion density (n_i) and T_i gradients. The difference in central toroidal speed (Δv_ϕ) is given by

$$\Delta v_\phi = \frac{T_i}{Z_i e B_p}\left[\alpha_1 \frac{d(\ln T_i)}{dr} + \alpha_2 \frac{d(\ln n_i)}{dr}\right], \qquad (2)$$

where Z_i is the charge number of the main ion species, e is the elementary charge, and B_p is the poloidal magnetic field. $\alpha_1 (=0.80)$ and $\alpha_2 (=0.57)$ are two constants which depend on the aspect ratio of the tokamak and on an impurity strength parameter which is a measure for the amount of impurities present in the plasma. Substituting all parameters, assuming $n_i = n_e$, a maximum value of $\Delta v_\phi = 1.0 \times 10^4$ ms^{-1} has been derived. Therefore, as a possible difference in rotation speed will be lost in the measurement noise, the experimental observations do not contradict the neoclassical results.

In conclusion, the results of measurements reported here show that it is possible to determine the toroidal rotation speed of the TEXTOR hydrogenic ions in a rather straightforward way by using the Rutherford scattering diagnostic. Detailed measurements on, e.g., the radial dependence of the toroidal speed and simultaneous measurements of the toroidal rotation of the hydrogenic and impurity ions are now possible. This enables comparison of the toroidal rotation speed of the various plasma ions with predictions from theoretic models.

The authors would like to thank S. A. H. Moorman for her assistance during the measurements, F. C. Schüller for his comments, and the TEXTOR team for their technical support and interest in the experiment. This work was performed as part of the research program of the association agreement of Euratom and the "Stichting voor Fundamenteel Onderzoek der materie" (FOM), with financial support from the "Nederlandse Organisatie voor Wetenschappelijk Onderzoek" (NWO) and Euratom.

[1] R. C. Isler *et al.*, Nucl. Fusion **23**, 1017 (1983).
[2] S. Suckewer *et al.*, Nucl. Fusion **24**, 815 (1984).
[3] N. C. Hawkes and N. J. Peacock, Nucl. Fusion **25**, 971 (1985).
[4] R. C. Isler *et al.*, Nucl. Fusion **26**, 391 (1986).
[5] H. Weisen *et al.*, Nucl. Fusion **29**, 2187 (1989).
[6] N. Nakajima and M. Okamoto, National Institute for Fusion Science Report No. NIFS-102, 1991 (unpublished).
[7] Y. B. Kim, P. H. Diamond, and R. J. Groebner, Phys. Fluids B **3**, 2050 (1991).
[8] K. H. Burrell, A. F. Lietzke, and M. J. Schaffer, IEEE Trans. Plasma Sci. **6**, 107 (1978).
[9] A. J. H. Donné, E. P. Barbian, and H. W. van der Ven, J. Appl. Phys. **62**, 3130 (1987).
[10] A. A. E. van Blokland *et al.*, Rev. Sci. Instrum. **63**, 3359 (1992).
[11] G. H. Wolf *et al.*, Plasma Phys. Controlled Fusion **28**, 1413 (1986).
[12] H. F. Tammen *et al.*, Rev. Sci. Instrum. **63**, 4583 (1992).
[13] A. J. H. Donné and F. J. de Heer, J. Appl. Phys. **62**, 780 (1987).
[14] S. Ishida *et al.*, Nucl. Fusion **28**, 2225 (1988).

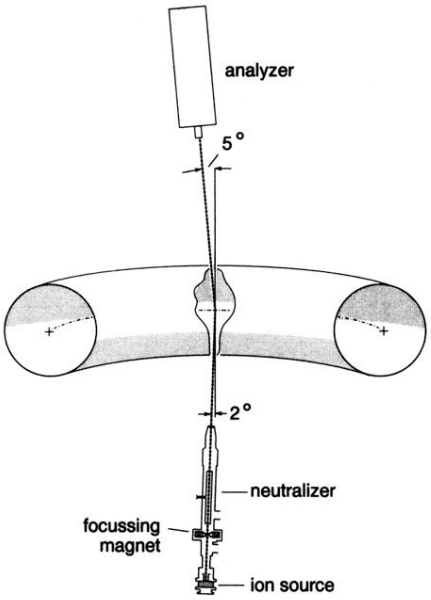

FIG. 1. Schematic view of the experimental setup of the Rutherford scattering diagnostic at TEXTOR.